Supporting information: Structural Control over Bimetallic Core-Shell Nanorods for Surface Enhanced Raman Spectroscopy

Jessi E.S. van der Hoeven[1,2,|,*], Tian-Song Deng[1,3,|,*], Wiebke Albrecht[1], Liselotte A. Olthof[1,2], Marijn A. van Huis[1], Petra E. de Jongh[2], and Alfons van Blaaderen[1,*]

[1]*Soft Condensed Matter, Debye Institute for Nanomaterials Science, Utrecht University, Princetonplein 5, 3584 CC Utrecht, The Netherlands*

[2]*Inorganic Chemistry and Catalysis, Debye Institute for Nanomaterials Science, Utrecht University, Universiteitsweg 99, 3584 CG Utrecht, The Netherlands*

[3]*Current address: School of Electronics and Information Engineering, Hangzhou Dianzi University, Hangzhou, 310018, China*

[|]Contributed equally to this work

[*]To whom correspondence should be addressed.

E-mail: j.e.s.vanderhoeven@uu.nl; dengts@pku.edu.cn; a.vanblaaderen@uu.nl

Supplementary Figures

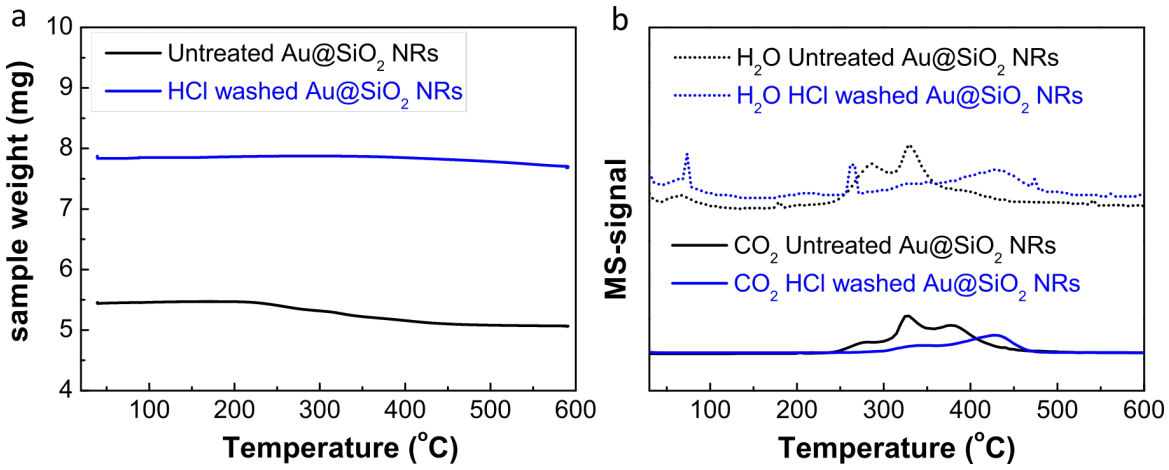

Figure S1: Thermogravimetric analysis (TGA) measurements on Au@SiO_2 NRs before and after the HCl-washing. a) TGA curves displaying the sample weight of untreated and 0.10 M HCl in EtOH washed Au@SiO_2 NRs as a function of the heating temperature. b) Mass spectrometry (MS) results corresponding to the TGA curves in a) showing the combustion products H_2O and CO_2 of CTAB as a function of the heating temperature. Both the TGA and MS results show that most of the CTAB was removed after HCl washing. The measurements were done with Au@SiO_2 NRs with $L_{Au} = 95 \pm 8$ nm, $D_{Au} = 26 \pm 2$ nm ($\lambda_{LSPR} = 795$ nm) and a ~18 nm thick mesoporous silica shell. The TGA-MS measurements were carried out in air.

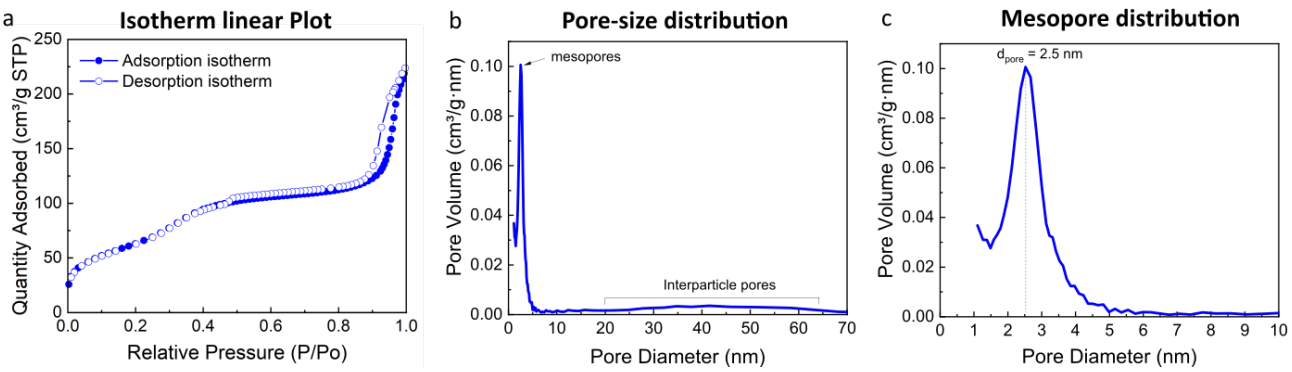

Figure S2: Quantification of the porosity of the silica shell using nitrogen physisorption. a) Isotherm linear plot showing the adsorption (closed symbols) and desorption isotherm (open symbols). The hysteresis between the adsorption and desorption isotherm at 0.9 to 1.0 relative pressure indicates the presence of mesopores. b) Pore size distribution showing the pore volume for different pore diameters. The broad peak from 20 to 60 nm is due to the pores between the nanorods. The peak at a pore diameter of 2.5 nm is caused by the mesopores in the silica shell, as is shown more clearly in panel c). The BET surface area was 235 m^2/g.

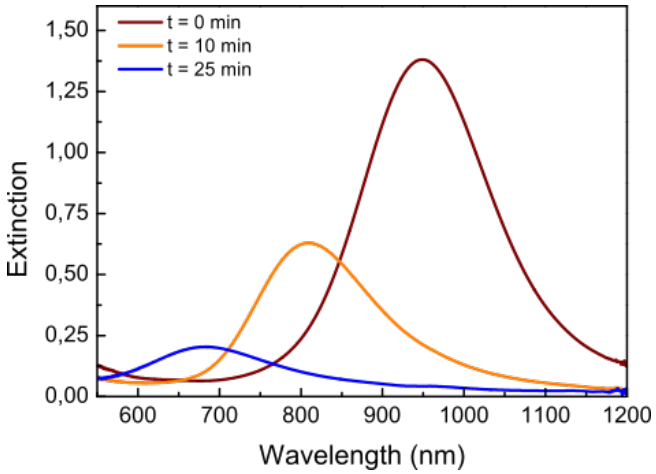

Figure S3: Extinction spectra of Au@SiO_2 NRs etched in the absence of CTAB. The optical spectra after 0, 10 and 25 min of etching correspond to the Au@SiO_2 NRs in the TEM images in Figure 1d of the main text. Upon etching the LSPR peak position changed from 950 (red), to 811 (orange), to 684 nm (blue).

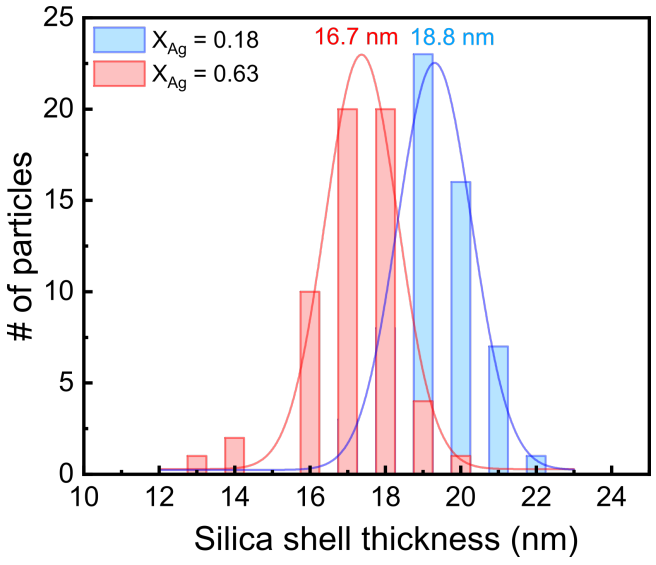

Figure S4: The silica shell thickness of Au@Ag@SiO_2 NRs decreases upon Ag-shell growth. The plot shows the distributions in silica shell thickness for Au@Ag@SiO_2 NRs with a thin ($X_{Ag} = 0.18$) and thick ($X_{Ag} = 0.63$) Ag-shell, which have an average silica shell thickness of 18.8 and 16.7 nm, respectively.

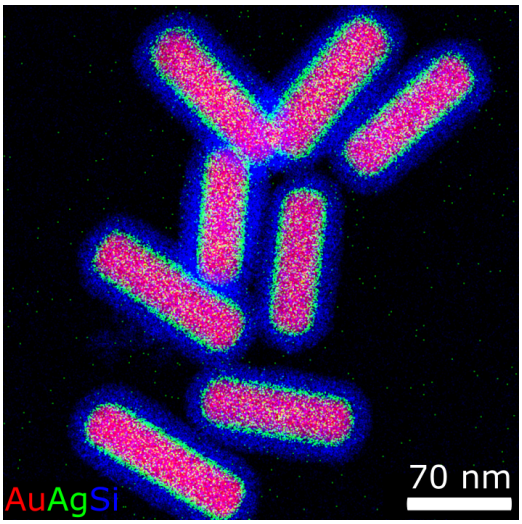

Figure S5: Direct Ag overgrowth on non-etched Au@SiO_2 NRs. EDX map of Au@Ag@SiO_2 NRs, where the Ag overgrowth was performed on non-etched Au@SiO_2 NRs after CTAB removal. The synthesis was performed on a 400 mL scale. $X_{Ag} = 0.24$, sample weight = 26 mg, metal loading = 85 wt%, $L = 107 \pm 9.7$ nm, $D = 35 \pm 2.9$ nm, $V = 9.1 \pm 1.9 \times 10^4$ nm^3.

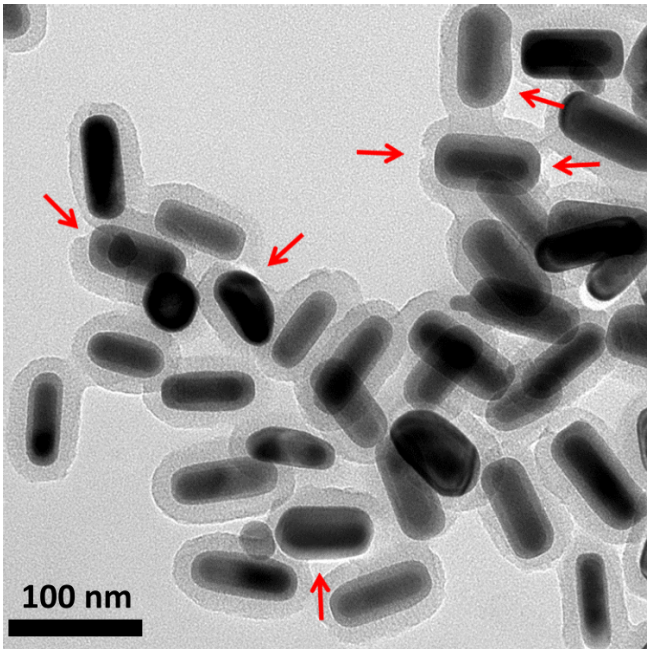

Figure S6: Excess Ag overgrowth on Au cores leads to cracking of the surrounding silica shells. The red arrows indicate the places cracks in the silica shell due to the expansion of bimetallic core. For the particles with the cracked shell the Ag shell had a 5 times larger volume than the Au core and was 3.5 times larger than the original Au rod before etching.

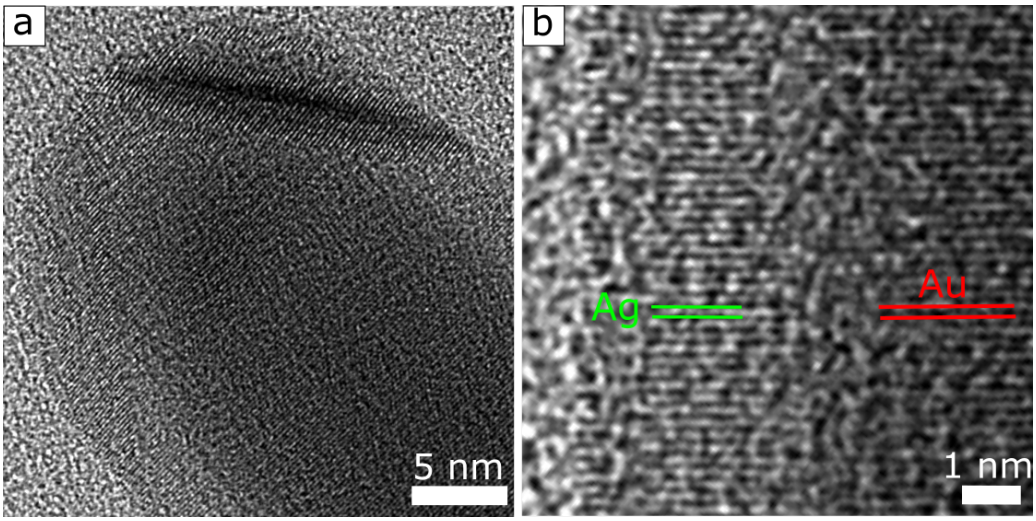

Figure S7: High resolution bright field TEM images of Au@Ag@SiO_2 NRs. a) HRTEM image and b) corresponding zoom-in of the Au@Ag@SiO_2 NR with $d^{Au}_{lattice}$= $d^{Ag}_{lattice}$= 0.205 nm, corresponding to {200} lattice planes.

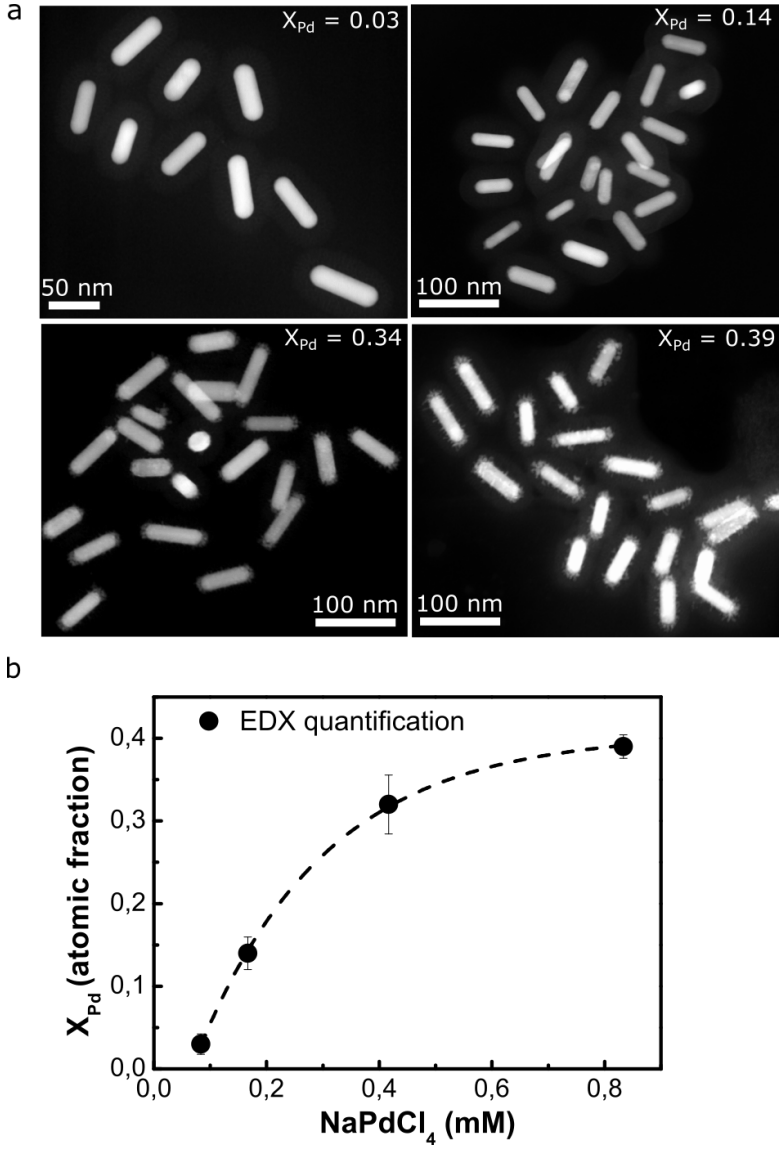

Figure S8: Overview of Au@Pd@SiO_2 NRs with X_{Pd} = 0.03-0.39 a) HAADF-STEM images of Au@Pd@SiO_2 NRs grown with 0.083-3.3 mM $NaPdCl_4$, yielding NRs with X_{Pd} = 0.03-0.39. b) Plot of the X_{Pd} versus the $NaPdCl_4$ concentration used in the metal overgrowth.

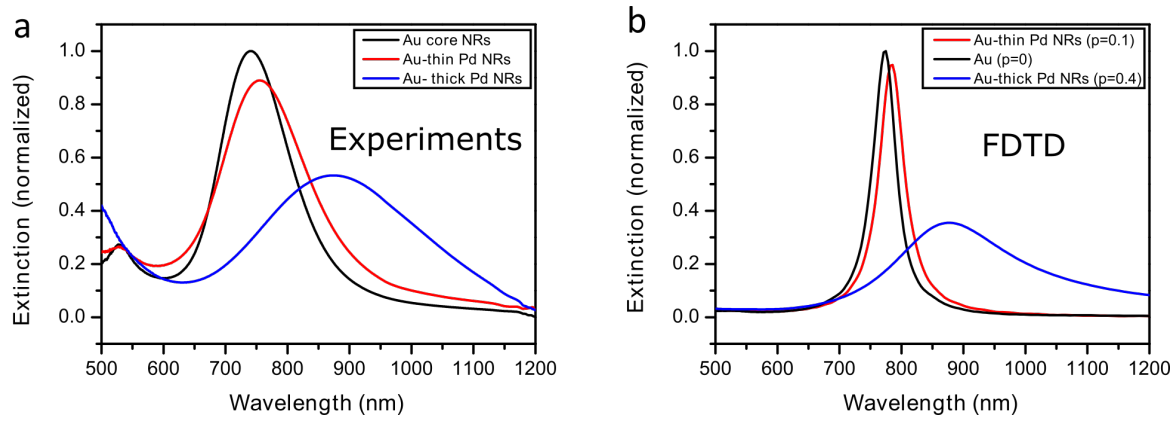

Figure S9: Comparison between the experimental and FDTD calculated spectra of Au@Pd@SiO_2 NRs with a thin and thick Pd shell a) Experimental spectra for 0.083 mM (red, L = 60.5 nm, D = 19.7 nm) and 0.83 mM (blue, L = 78.6 nm, D = 19.4 nm) Na_2PdCl_4. The extinction of the Au@Pd@SiO_2 NRs spectra was normalized with respect to the extinction spectrum of the Au core NRs (black, L = 58.5 nm, D = 17.7 nm). The spectrum of the Au@Pd@SiO_2 NRs grown with 0.83 mM Na_2PdCl_4 has an offset of -0.2 (along the y-axis) for better comparison. (b) FDTD calculated spectra with a Pd volume fraction of $p = 0.1$ (red) and $p = 0.4$ (blue) match the the experimental spectra in a) best. Hence, the experimentally obtained Au@Pd@SiO_2 NRs have a discontinuous Pd shell.

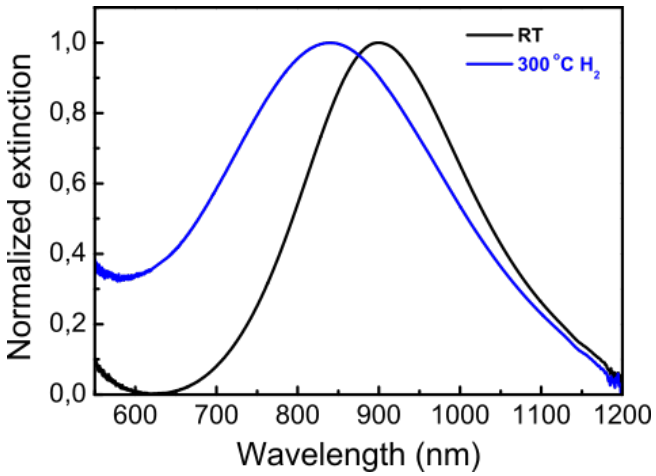

Figure S10: The plasmonic properties of Au@Pd@SiO_2 NRs change upon thermal treatment indicating a change in Pd shell morphology. Black: extinction spectra of the as prepared Au@Pd@SiO_2. Corresponding TEM images of this sample are shown in Figure 3f. Blue: extinction spectrum of the Au@Pd@SiO_2 NR after thermal treatment in H_2 at 300 °C. Corresponding TEM images of this sample are shown in Figure 3g. Thermal treatment led to a blue shift of the LSPR from 899 nm to 840 nm, indicating a transition from a discontinuous to a continuous Pd shell

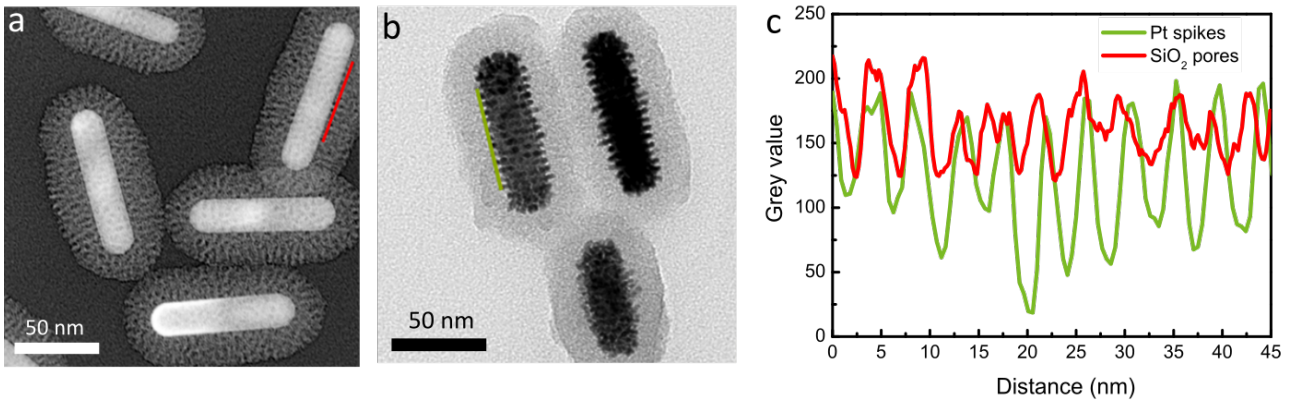

Figure S11: TEM investigation of the pore structure before and after Pt overgrowth. a) TEM image of mesoporous silica coated AuNR as prepared, and b) after Pt overgrowth. A line scan was performed along the red (a) and green (b) line. The grey values as a function of distance are plotted in panel c. The periodicity in grey values before and after overgrowth is similar indicating that no large changes in the mesopore structure occurred upon Pt overgrowth

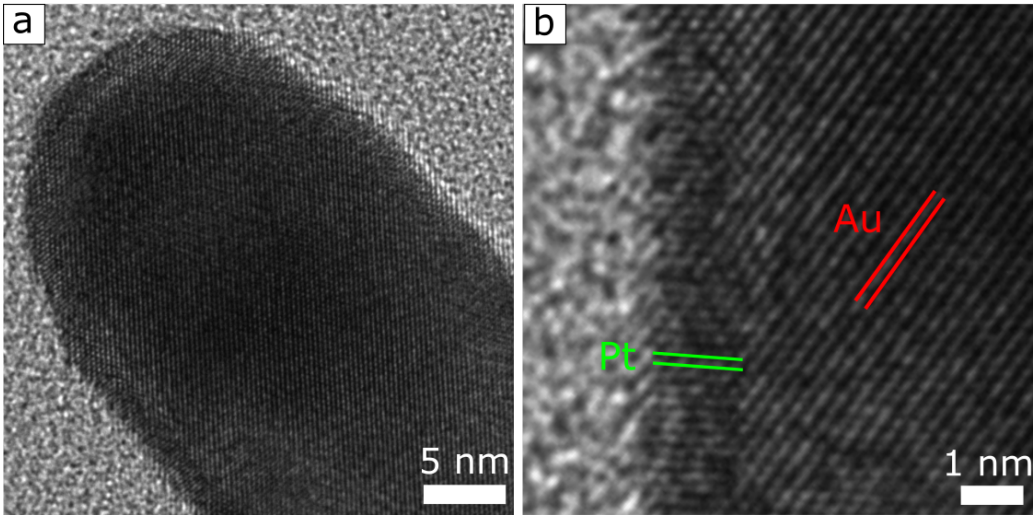

Figure S12: High resolution bright field TEM images of Au@Pt@SiO_2 NRs. a) HRTEM image and b) corresponding zoom-in of the Au@Pt@SiO_2 NR with $d^{Au}_{lattice}$= 0.237 nm and $d^{Pt}_{lattice}$= 0.22 nm, corresponding to the (111) lattice planes.

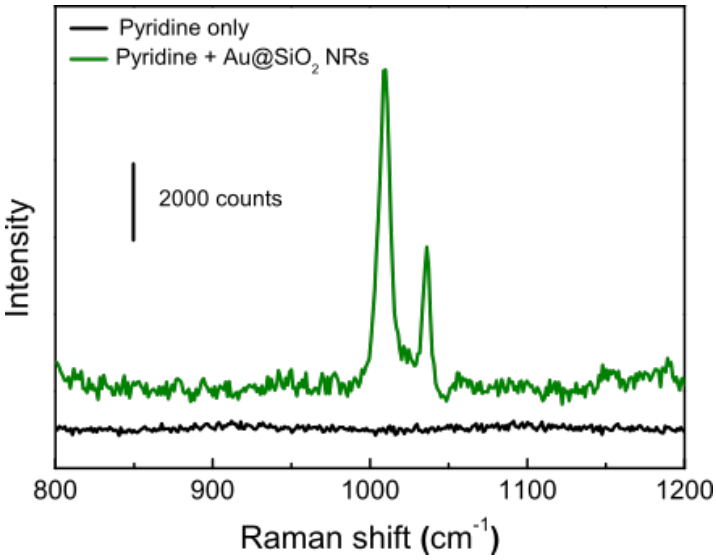

Figure S13: Verifying the accessibility of silica coated AuNRs after CTAB removal from the mesopores using pyridine SERS. Raman spectra of pyridine (10 mM in H_2O) with Au@SiO_2 NRs (green) and without (black). The spectra were recorded using a 50× air objective and a 633 nm laser operating at a laser power of 1.3 mW. A measurement time of 1 s was used

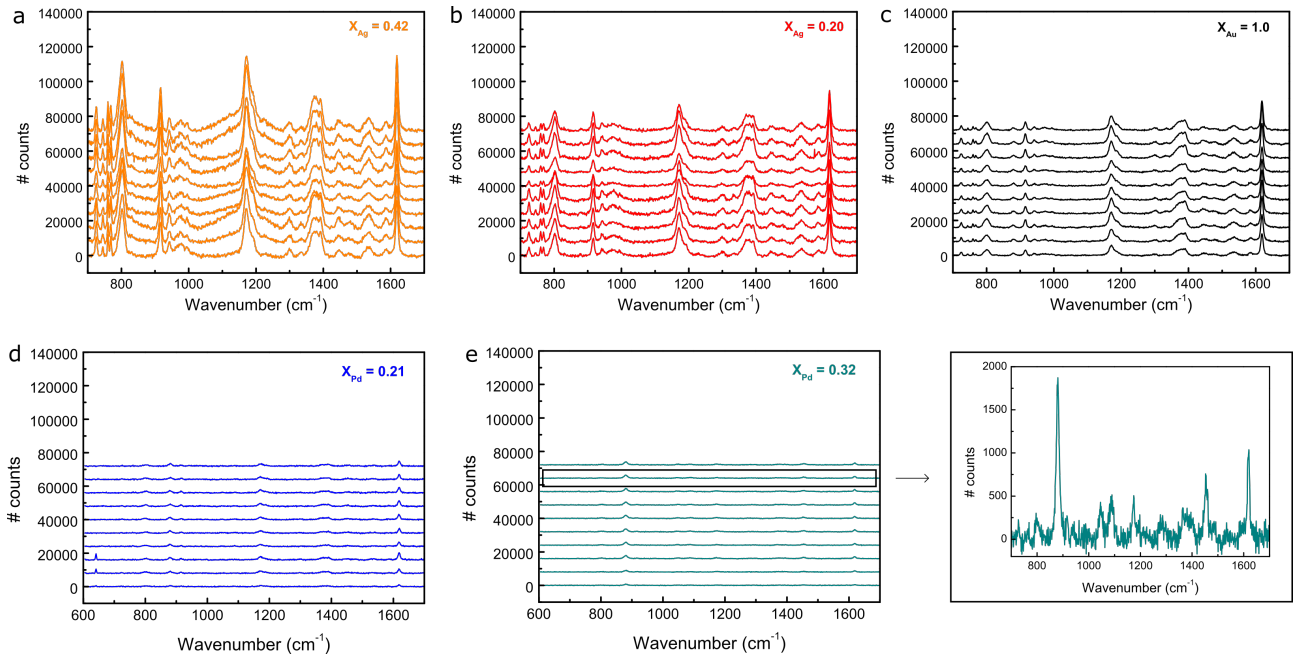

Figure S14: Reproducible SERS measurements of crystal violet (CV) in the presence of bimetallic Au@Ag@SiO_2 and Au@Pd@SiO_2 NRs, and monometallic Au@SiO_2 NRs measured at 10 different positions in each capillary. The CV concentration was 1.0 μM in a 3:1 EtOH:H_2O mixture containing a constant metal concentration of [Au] = 0.5 mM. As the Au core sizes are similar (V_{core}= 1.2-2.4×10^4) the particle density is comparable in the different samples. The resulting spectra of Au@Ag@SiO_2 NRs with X_{Ag} = 0.42 (a) and 0.20 (b), Au@SiO_2 NRs with X_{Au} = 1.0 (c) and Au@Pd@SiO_2 NRs with X_{Pd} = 0.21 (d) and 0.32 (e) are shown in orange, red, black, blue and turquoise, respectively.

Supplementary Tables

Table S1: Dimensions of the Au@Ag@SiO_2 NRs. For the overgrowth 0.300 mL etched AuNRs@meso-SiO_2 (L = 61.7 nm, D = 18.2 nm, LSPR = 748 nm, Ext= 2.2) in H_2O were used. The full set of reaction conditions used in the synthesis of the Au@Ag@SiO_2 NRs are presented in Table 2. The size parameters are based on TEM analysis of 100 particles per sample.

X_{Ag}	$AgNO_3$ (mM)	Length (nm)	Diameter (nm)	AR
0	0	61.7±9.7	18.2±2.2	3.4±0.5
0.18	0.05	64.5±9.8	19.7±2.1	3.3±0.5
0.35	0.08	64.3±9.9	22.2±2.7	2.9±0.4
0.41	0.13	68.4±11	22.7±2.4	3.0±0.5
0.50	0.17	72.9±11	23.9±2.5	3.0±0.4
0.57	0.22	75.5±11	25.3±3.2	3.0±0.4
0.57	0.27	75.6±11	25.3±3.2	3.0±0.3
0.61	0.30	76.7±10	26.6±2.8	2.9±0.4
0.63	0.33	75.7±10	27.4±3.5	2.8±0.4

Table S2: Ag overgrowth: reaction conditions used for the Au@Ag@SiO_2 NRs presented in Figure 2 in the main text. For the overgrowth 0.300 mL etched AuNRs@meso-SiO_2 (length (L)= 61.7 nm; diameter (D)= 18.2 nm, λ_{LSPR}= 748 nm, Ext= 2.2) in H_2O were used. Reaction time = 20 min. $AgNO_3$/Ascorbic acid (added) and $AgNO_3$/Ascorbic acid (final) refer to the amount and concentration of the $AgNO_3$/Ascorbic acid solution added to the reaction mixture, and the final $AgNO_3$/Ascorbic acid concentration in the reaction mixture, respectively.

X_{Ag}	$AgNO_3$ (added)	Ascorbic acid (added)	$AgNO_3$ (final)	Ascorbic acid (final)
0.18	0.015 mL 1.0 mM	0.015 mL 4.0 mM	0.045 mM	0.18 mM
0.35	0.030 mL 1.0 mM	0.030 mL 4.0 mM	0.083 mM	0.33 mM
0.41	0.023 mL 2.0 mM	0.023 mL 8.0 mM	0.13 mM	0.53 mM
0.50	0.030 mL 2.0 mM	0.030 mL 8.0 mM	0.17 mM	0.67 mM
0.57	0.019 mL 4.0 mM	0.019 mL 16 mM	0.22 mM	0.90 mM
0.57	0.023 mL 4.0 mM	0.023 mL 16 mM	0.27 mM	1.1 mM
0.61	0.026 mL 4.0 mM	0.026 mL 16 mM	0.30 mM	1.2 mM
0.63	0.030 mL 4.0 mM	0.030 mL 16 mM	0.33 mM	1.3 mM

Table S3: Pd overgrowth: reaction conditions used for the Au@Pd@SiO_2 NRs presented in Figure 3 in the main text. For the overgrowth 0.300 mL etched AuNRs@meso-SiO_2 (L= 60.8 nm, D= 19.5 nm, λ_{LSPR}= 746 nm, Ext= 2.2) in H_2O were used. Reaction time = 20 min. Na_2PdCl_4/Ascorbic acid (added) and Na_2PdCl_4/Ascorbic acid (final) refer to the amount and concentration of the Na_2PdCl_4/Ascorbic acid solution added to the reaction mixture, and the final Na_2PdCl_4/Ascorbic acid concentration in the reaction mixture, respectively.

X_{Pd}	Na_2PdCl_4 (added)	Ascorbic acid (added)	Na_2PdCl_4 (final)	Ascorbic Acid (final)
0.03	0.030 mL 1.0 mM	0.030 mL 4.0 mM	0.083 mM	0.33 mM
0.14	0.030 mL 2.0 mM	0.030 mL 8.0 mM	0.17 mM	0.67 mM
0.34	0.030 mL 5.0 mM	0.030 mL 20 mM	0.42 mM	1.7 mM
0.39	0.030 mL 10 mM	0.030 mL 40 mM	0.83 mM	3.3 mM

Table S4: Pt overgrowth: reaction conditions used for the Au@Pt@SiO_2 NRs presented in Figure 4 in the main text. For the overgrowth 0.300 mL etched AuNRs@meso-SiO_2 (L= 61.7 nm, D= 18.2 nm, λ_{LSPR}= 748 nm, Ext= 2.2) in H_2O were used. The reaction mixture was left overnight. K_2PtCl_4/Ascorbic acid (added) and K_2PtCl_4/Ascorbic acid (final) refer to the amount and concentration of the K_2PtCl_4/Ascorbic acid solution added to the reaction mixture, and the final K_2PtCl_4/Ascorbic acid concentration in the reaction mixture, respectively.

K_2PtCl_4 (added)	Ascorbic acid (added)	K_2PtCl_4 (final)	Ascorbic acid (final)
0.030 mL 1.0 mM	0.030 mL 4.0 mM	0.083 mM	0.33 mM
0.030 mL 10 mM	0.030 mL 40 mM	0.83 mM	3.3 mM
0.030 mL 50 mM	0.030 mL 200 mM	4.2 mM	17 mM
0.030 mL 100 mM	0.030 mL 400 mM	8.3 mM	33 mM

Table S5: Estimated yield in Ag overgrowth. Based on the metal concentrations used in the metal overgrowth, the theoretical composition (X_{Ag} calculated) was estimated and compared to the measured composition (X_{Ag} measured). The yield is the measured composition divided by the calculated composition times 100 %. The gold concentration in the 0.3 mL dispersion used in the metal overgrowth step was estimated to be 0.18 mM. This estimate is based on the following assumptions: i) in the AuNR synthesis: [$HAuCl_4$] = 0.5 mM, ii) in the AuNR synthesis: [Au^0] = 0.33 mM (which is based on the fact that only 2/3 of the $HAuCl_4$ is reduced as [ascorbic acid] = 0.33 x [Au^{1+}], and 1 ascorbic acid molecule can reduce 2 Au^{1+} ions to Au^0), iii) in the metal overgrowth: [Au^0] = 0.18 mM, as the Au concentration used in the metal overgrowth is 0.55 times the Au concentration used during the AuNR synthesis.

$AgNO_3$ (added)	Au (added)	X_{Ag} calculated	X_{Ag} measured	Yield (%)
0.015 μmol	0.054 μmol	0.22	0.18	83
0.030 μmol	0.054 μmol	0.36	0.35	98
0.045 μmol	0.054 μmol	0.45	0.41	90
0.060 μmol	0.054 μmol	0.53	0.50	95
0.075 μmol	0.054 μmol	0.58	0.57	98
0.090 μmol	0.054 μmol	0.63	0.57	91
0.0105 μmol	0.054 μmol	0.66	0.61	92
0.012 μmol	0.054 μmol	0.68	0.63	91

Table S6: Estimated yield in Pd overgrowth. Based on the metal concentrations used in the metal overgrowth, the theoretical composition (X_{Pd} calculated) was estimated and compared to the measured composition (X_{Pd} measured). The yield is the measured composition divided by the calculated composition times 100 %. The gold concentration in the 0.3 mL dispersion used in the metal overgrowth step was estimated to be 0.18 mM.

Na_2PdCl_4 (added)	Au (added)	X_{Pd} (calculated)	X_{Pd} (measured)	Yield (%)
0.030 μmol	0.054 μmol	0.36	0.03	8
0.060 μmol	0.054 μmol	0.53	0.14	27
0.15 μmol	0.054 μmol	0.74	0.34	46
0.30 μmol	0.054 μmol	0.85	0.39	46

Table S7: Sample details Au@Ag@SiO_2, Au@SiO_2 and Au@Pd@SiO_2 NRs used for the SERS measurements as presented in Figure 6 in the main text. The composition of the particles was determined via ICP and the particle dimensions via TEM. The values are an average of 50-100 size measurements per particle batch. The composition was determined using ICP. The error in the given compositions is $\leq$3%.

Composition	Length (nm)	Diameter (nm)	Aspect ratio	Particle volume (10^4 nm^3)	Au core volume (10^4 nm^3)
$X_{Au} = 1.0$	67±6.3	19±2.2	3.5±0.5	1.8±0.5	1.8±0.4
$X_{Ag} = 0.20$	73±6.8	26±3.1	2.8±0.4	3.5±0.9	2.5±0.5
$X_{Ag} = 0.42$	75±6.3	30±3.0	2.5±0.3	4.6±0.9	2.5±0.5
$X_{Pd} = 0.21$	65±6.4	19±1.8	3.5±0.5	1.6±0.4	1.2±0.3
$X_{Pd} = 0.32$	72±7.7	24±3.2	3.5±0.4	2.9±0.9	2.0±0.6

Table S8: **Maximum local field E_{max} computed with FDTD around Au@SiO_2, Au@Ag@SiO_2 and Au@Pd@SiO_2 NRs** in the xz direction, where the z-axis is directed along the length of the NR.

Composition	E_{xz}^{max}
$X_{Ag} = 0.42$	3396
$X_{Ag} = 0.20$	198
$X_{Au} = 1.0$	12
$X_{Pd} = 0.21$	14
$X_{Pd} = 0.32$	22